Building and Environment, Vol. 24, No. 1, pp. 23–32, 1989.
Printed in Great Britain.

0360–1323/89 $3.00+0.00

Simulation of Air Flow About a Directly Air Cooled Heat Exchanger

WILLEM A. SCHREÜDER*
J. PRIEUR DU PLESSIS†

The flow of air about a very large directly air cooled heat exchanger is simulated numerically. Air is forced through the heat exchanger by fans and a strongly buoyant plume is formed. The numerical treatment uses a finite difference technique combined with special treatment of atmospheric boundaries. It restricts the computational domain to manageable limits by allowing boundaries with moderate in and outflow to be specified in terms of gradient boundary conditions. The influence of adverse wind conditions on the heat transfer and plume behaviour is examined.

NOMENCLATURE

a	finite volume coefficient
C_p	heat capacity
C_t	low Reynolds number k–ε generation term
C_1	turbulence parameter
C_2	turbulence parameter
$C_{2\infty}$	turbulence parameter
C_μ	turbulence parameter
$C_{\mu\infty}$	turbulence parameter
E_t	shear turbulence dissipation term
G_p	shear momentum generation term
G_T	shear heat generation term
G_t	shear turbulence generation term
k	turbulent kinetic energy
p	pressure
R_t	turbulent Reynolds number
T	temperature
u	horizontal velocity
v	vertical velocity
x	horizontal distance
y	vertical distance
ε	turbulent kinetic energy dissipation rate
ρ	density
μ	laminar viscosity
μ_t	turbulent viscosity
σ_T	turbulent Prandtl number for temperature
σ_k	turbulent Prandtl number for k
σ_ε	turbulent Prandtl number for ε

Subscripts

amb	ambient outside numerical domain
bnd	on the numerical boundary
E, W, N, S	east (right), west (left), north (top), south (bottom)
int	interior of the numerical domain.

1. INTRODUCTION

THE FLOW of air through and around a directly air cooled heat exchanger has many practical implications. The high cost of experimental models makes numerical investigations of the problem an important part of the design process. The SIMPLE family of methods is a popular choice, in part because all are primitive variable methods. It is therefore possible to model complex structures and boundary conditions with reasonable ease. The treatment of atmospheric boundaries does require special care, but a practical procedure for their treatment has been developed by the authors [1].

The particular problem investigated concerns a very large heat exchanger construction as found at a power station. The heat exchanger panels are arranged horizontally on an elevated structure next to the power station buildings. Air is forced through the heat exchanger by large fans at a speed in the order of 5 m s^{-1}. The heat exchanger assembly is capable of dissipating in the order of 1000 MW at normal operating temperatures. A heat exchanger of this size clearly has a large influence on the atmospheric conditions in the vicinity of the structure. Two significant features are expected to dominate the flow pattern, namely a strongly buoyant plume emanating from the heat exchanger and an induction funnel drawing air in below the heat exchanger structure. There is, however, a real danger that under adverse conditions a so-called "heat island" may form when the heat exchanger ingests the plume of warm air it exhausts and forms a closed circuit of warm air around itself. This would cause relatively little heat to be dissipated, rendering the heat exchanger virtually useless. This problem could be caused by such conditions as strong wind or a severe temperature inversion. Part of this investigation is to examine the effects of these atmospheric conditions.

A FORTRAN code called JEEP was developed to solve the problem. The problem is modelled using the SIMPLEB method of the authors [1], a derivative of the SIMPLE family of methods. One of the disadvantages of the SIMPLE type methods is that, unless a coordinate transformation is done, a finite computational domain must be used.

The chosen computational domain used here is a rectangular, 2-D vertical flat plane through the heat exchanger, with atmospheric boundaries on two adjacent

*Department of Mathematics, West Virginia University, Morgantown, WV 26506, U.S.A.
†Centre for Numerical Thermoflow, Department of Mechanical Engineering, University of Pretoria, Pretoria, 0002, South Africa.

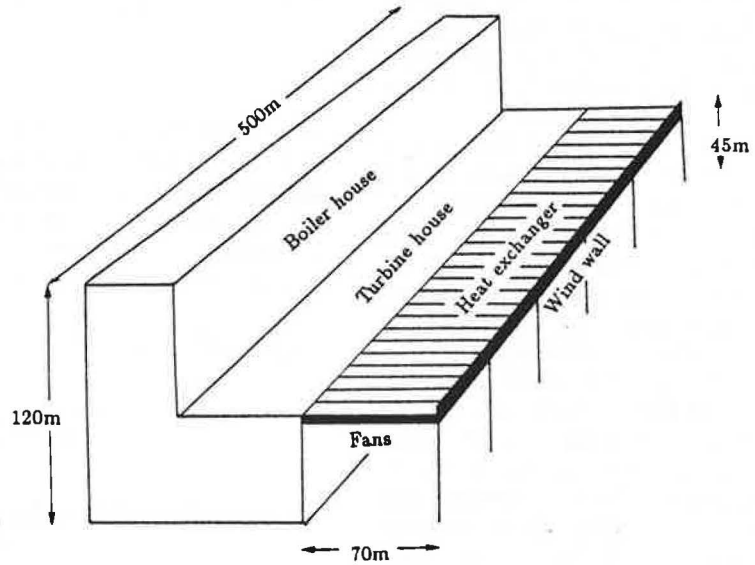

Fig. 1. Schematic presentation of the power station.

sides, the ground surface on the third and a special upwind boundary on the last side. The atmospheric boundary conditions are important since it is anticipated that the plume from the heat exchanger will be strongly buoyant. The heat exchanger will therefore have to draw in air over the major part of the atmospheric boundaries at a velocity of the order of 1 m s^{-1}. These boundaries are treated using a half cell method [1] which allows the atmospheric boundaries to be specified largely in terms of gradient boundary conditions.

The continuity, momentum and energy equations are used in their fully elliptic form to model mass and heat transfer in the computational domain. High turbulence levels are anticipated in the vicinity of the heat exchanger. The k–ε turbulence model is used to predict turbulence levels.

2. PHYSICAL PROBLEM

The power station is shown schematically in Fig. 1. The structure is quite large, the boiler house being approximately 120 m high and the turbine house about 45 m high. The fan/heat exchanger assembly extends about 70 m outward from the roof of the turbine house and is about 10 m thick. The heat exchanger itself actually consists of finned tube heat exchanger panels, arranged in a series of A-frame constructions running outward from the turbine building. The fans are mounted below it. The whole structure is in the order of 500 m long, giving the heat exchanger a planform area of about 35,000 m^2. The turbine building and heat exchanger structure extends continuously for the full length of the complex, but the boiler house in Fig. 1 actually represents six boiler houses that are approximately square in planform. The average height of the boiler house array is about 100 m.

The heat exchanger receives the low pressure steam directly from the low pressure turbine, but the effective fin temperature during normal operating conditions is only about 50°C. With an effective inlet air temperature of about 20°C and an outlet air temperature close to the fin temperature, this implies a change in the absolute air temperature (and therefore also the density) of about 10%. It is clear that buoyancy will be a very important effect even though the fans render it primarily a system driven by forced convection.

Air is forced upward through the heat exchanger, so that air is drawn in below the fan/heat exchanger assembly. The turbine house seals off the one end of the volume below the heat exchanger, so that, due to the comparatively small lateral open ends of the structure, the air must be drawn in underneath the end of the heat exchanger furthest from the turbine house. It is clear that the strong induction under the heat exchanger will draw with it some of the air that has already passed through the heat exchanger round the far end. This recirculation will reduce the effectiveness of the heat exchanger, because the effective inlet air temperature will be higher as a result of this warm air. The worst case would be if the plume is totally bent over towards the inlet by, for example, wind or a temperature inversion and thus ingested by the strong induction caused by the fans. This results in a "heat island" where practically the same mass of air is continuously pumped through the heat exchanger. This whole air mass would be approximately at the temperature of the heat exchanger so that very little or no heat is transferred to it. The amount of heat transferred wil be determined by how much heat is being transferred from the recirculating heat mass to the surrounding air by conduction and convection. This secondary process is very ineffective compared to the transfer of heat from the heat exchanger to the air at the ambient air temperature. In the latter case the buoyant plume also helps to carry the energy away from the site.

To reduce this recirculation, a so-called wind wall is constructed along the edge of the heat exchanger assembly as shown in Fig. 1. It consists of a solid metal sheet with a supporting structure. The wind wall extends above the top of the heat exchanger to block the path of exhaust air that would have flowed round the edge of the

heat exchanger structure, to be drawn in by the fans. Approximately one metre at the ends of the A-frames, does not consist of heat exchanger panels, but is a supporting structure that is sealed off so that air cannot escape there, forcing it to flow through the heat exchanger panels.

Qualitatively, therefore, the expected flow pattern would comprise of a strongly buoyant plume extending from the heat exchanger upwards to a considerable altitude, together with a funnel-like in-flow pattern converging on the edge of the fan/heat exchanger assembly. In between these predominant features there will be some recirculation, air being diverted from the edge of the plume around the wind wall to the inlet area. The recirculation pattern may be on a small scale with air flowing closely around the wind wall, or large scale with air diverting from the plume and flowing into the induction area some distance away from the heat exchanger assembly. From the expected flow rate, however, it is clear that there will be areas of high shear, especially around the inlet and outlet of the heat exchanger assembly. It is expected that high turbulence levels will be found in these regions.

3. NUMERICAL MODEL

The length of the heat exchanger is an order of magnitude greater than its width and height, and it is therefore assumed that the problem can be reasonably well approximated in two dimensions. It is further assumed that there are no time-dependent effects. This considerably decreases the computational complexity of the problem. Note that from the qualitative flow pattern described in the previous section there is no predominant flow direction for the whole domain. The equations are therefore used in their steady state, Cartesian, fully elliptic form.

Air is assumed to be an ideal gas and the relationship between the pressure, density and temperature is given by the equation of state $p = \rho R T$. The equations used to predict the horizontal (x-direction) velocity (u), vertical (y-direction) velocity (v), pressure (p) and temperature (T) are the continuity equation:

$$\frac{\partial}{\partial x}(\rho u) + \frac{\partial}{\partial y}(\rho v) = 0, \tag{1}$$

the momentum equations:

$$\rho u\frac{\partial u}{\partial x} + \rho v\frac{\partial u}{\partial y} = \frac{\partial}{\partial x}\left((\mu+\mu_t)\frac{\partial u}{\partial x}\right) + \frac{\partial}{\partial y}\left((\mu+\mu_t)\frac{\partial u}{\partial y}\right) - \frac{\partial p}{\partial x} - \frac{\partial G_\rho}{\partial x},$$

$$\rho u\frac{\partial v}{\partial x} + \rho v\frac{\partial v}{\partial y} = \frac{\partial}{\partial x}\left((\mu+\mu_t)\frac{\partial v}{\partial x}\right) + \frac{\partial}{\partial y}\left((\mu+\mu_t)\frac{\partial v}{\partial y}\right) - \frac{\partial p}{\partial y} - \rho g - \frac{\partial G_\rho}{\partial y}, \tag{2}$$

and the energy equation:

$$C_p\left[\rho u\frac{\partial T}{\partial x} + \rho v\frac{\partial T}{\partial y}\right] = \left(k + \frac{C_p\mu_t}{\sigma_T}\right)\left(\frac{\partial^2 T}{\partial x^2} + \frac{\partial^2 T}{\partial y^2}\right) + u\frac{\partial p}{\partial x} + v\frac{\partial p}{\partial y} + \mu G_T. \tag{3}$$

It is assumed that the heat capacity of the air (C_p) is constant. As argued above, high turbulence levels are anticipated. The k–ε turbulence model is a good compromise between simplicity and accuracy. The turbulent kinetic energy (k) and turbulent kinetic energy dissipation rate (ε) are modelled by the following equations:

$$\rho u\frac{\partial k}{\partial x} + \rho v\frac{\partial k}{\partial y} = \frac{\partial}{\partial x}\left(\left(\mu + \frac{\mu_t}{\sigma_k}\right)\frac{\partial k}{\partial x}\right) + \frac{\partial}{\partial y}\left(\left(\mu + \frac{\mu_t}{\sigma_k}\right)\frac{\partial k}{\partial y}\right) + \mu_t G_t - \rho\varepsilon - 2\mu C_t,$$

$$\rho u\frac{\partial \varepsilon}{\partial x} + \rho v\frac{\partial \varepsilon}{\partial y} = \frac{\partial}{\partial x}\left(\left(\mu + \frac{\mu_t}{\sigma_\varepsilon}\right)\frac{\partial \varepsilon}{\partial x}\right) + \frac{\partial}{\partial y}\left(\left(\mu + \frac{\mu_t}{\sigma_\varepsilon}\right)\frac{\partial \varepsilon}{\partial y}\right) + C_1 C_\mu \rho k G_t - \frac{C_2\rho\varepsilon^2}{k} + \frac{2\mu\mu_t}{\rho}E_t. \tag{4}$$

The shear related source terms in Equations (1)–(4) are:

$$G_\rho = \frac{2}{3}\left(\mu\frac{\partial u}{\partial x} + \mu\frac{\partial v}{\partial y}\right),$$

$$G_T = \frac{4}{3}\left(\frac{\partial u}{\partial x}\right)^2 + \left(\frac{\partial u}{\partial y}\right)^2 + \frac{2}{3}\left(\frac{\partial u}{\partial y}\frac{\partial v}{\partial x}\right) + \left(\frac{\partial v}{\partial x}\right)^2 + \frac{4}{3}\left(\frac{\partial v}{\partial y}\right)^2,$$

$$G_t = 2\left(\frac{\partial u}{\partial x}\right)^2 + \left(\frac{\partial u}{\partial y}\right)^2 + 2\left(\frac{\partial u}{\partial y}\frac{\partial v}{\partial x}\right) + \left(\frac{\partial v}{\partial x}\right)^2 + 2\left(\frac{\partial v}{\partial y}\right)^2,$$

$$E_t = \left(\frac{\partial^2 u}{\partial x^2}\right)^2 + 2\left(\frac{\partial^2 u}{\partial x\partial y}\right)^2 + \left(\frac{\partial^2 u}{\partial y^2}\right)^2 + \left(\frac{\partial^2 v}{\partial x^2}\right)^2 + 2\left(\frac{\partial^2 v}{\partial x\partial y}\right)^2 + \left(\frac{\partial^2 v}{\partial y^2}\right)^2,$$

$$C_t = \left(\frac{\partial\sqrt{k}}{\partial x}\right)^2 + \left(\frac{\partial\sqrt{k}}{\partial y}\right)^2.$$

Note that if ρ is a constant, the continuity equation requires that $G_\rho = 0$, so that the G_ρ term will only be significant if large density changes take place over a short distance. Note also that C_t is, strictly speaking, not a shear term, but a source term in the low Reynolds number k–ε turbulence model.

The turbulent viscosity (μ_t) and turbulent Reynolds number are defined as:

$$\mu_t = \frac{C_\mu\rho k^2}{\varepsilon} \quad \text{and} \quad R_t = \frac{\rho k^2}{\mu\varepsilon}.$$

Jones and Launder [2] showed that the turbulence parameters C_μ and C_2 depend on R_t, namely:

$$C_\mu = C_{\mu\infty}\exp\left(\frac{-2.5}{1+R_t/50}\right) \quad \text{and}$$

$$C_2 = C_{2\infty}(1-0.3\exp(-R_t^2)),$$

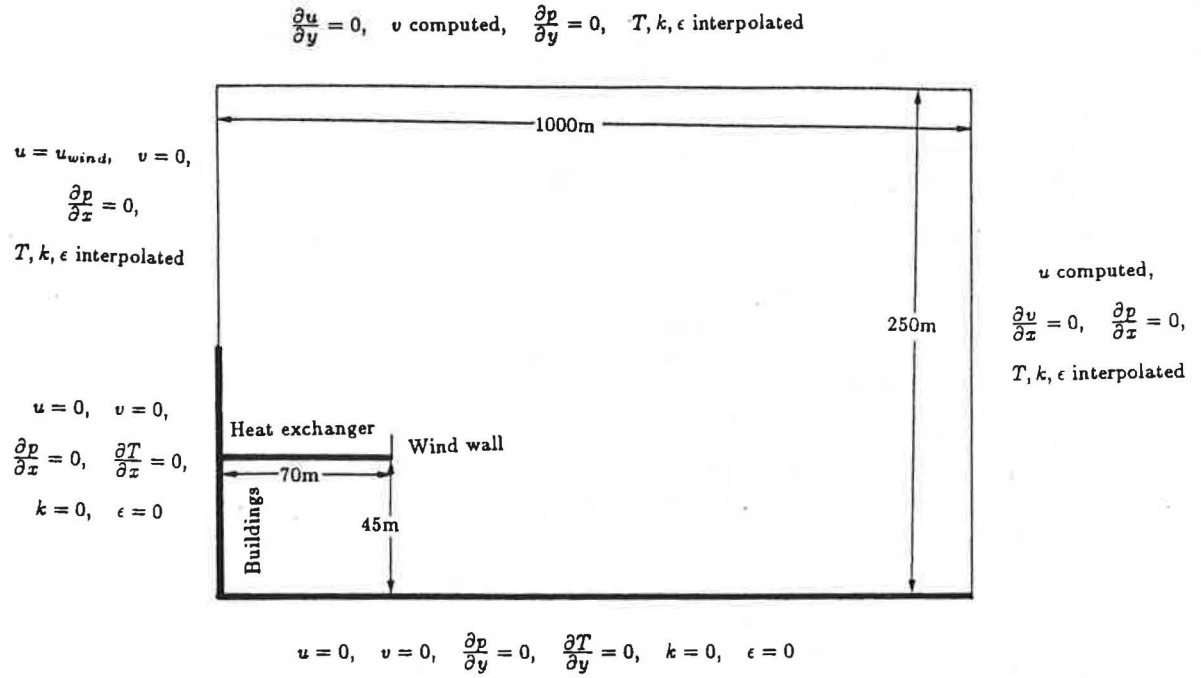

Fig. 2. Boundary conditions.

where $C_{\mu\infty} = 0.09$ and $C_{2\infty} = 1.92$. The parameter C_1 does not vary with R_t and $C_1 = 1.44$ is used.

The above equations are discretized on an L-wise staggered grid in the usual way as described by, for example, Patankar [3] and solved using the SIMPLEB method. The coefficients are approximated with the up-wind weighted differencing scheme (UWDS). The source terms are linearized as recommended by Patankar [3].

4. BOUNDARY CONDITIONS

The numerical domain used to solve the problem is shown in Fig. 2. The size of the domain was fixed at 1000 m horizontally and 250 m vertically. The left hand numerical boundary was chosen to be where the heat exchanger is attached to the building to eliminate the computational complexity of the flow over the power station buildings. Figure 2 summarizes the boundary conditions used.

A wind of significant speed is assumed from west to east across the power station complex. This makes it possible to specify values on the upward boundary that will not to any significant extent, be affected by the plume from the power station. A very important consequence of the 2-D assumption is that, if the plume remains buoyant, it becomes a barrier which the prevailing wind may not be able to penetrate. The plume will obviously be inclined away from the prevailing wind, but the domain downwind from the plume is effectively shielded from the wind. Flow in that region of the domain will be in the opposite direction to the wind. In practice the wind will be able to blow around the plume, but this is not possible in a 2-D model. The numerical boundaries are therefore treated as follows: the bottom (southern) boundary is the ground surface and is treated as a smooth solid structure, the upwind (western) boundary is part solid structure and the remainder prescribed by a given velocity distribution. The other (northern and eastern) boundaries are atmospheric boundaries and will require special treatment as is described below.

To model the collective effect of nearby buildings in the power station complex, a solid wall extending from ground level up to or higher than the heat exchanger is assumed for the lower portion of the western numerical boundary. Above this wall a constant, horizontal wind is assumed, $u = u_{wind}$ and $v = 0$. This is not strictly correct, as it is impossible to represent the variation in the height of the buildings along the complex in only two dimensions. This is to a certain extent compensated for by the buoyant plume. The plume effectively isolates the two domains on opposite sides of itself, so that the major effect of the wind as specified on the upwind boundary is to incline the plume towards the downwind side. The actual velocity distribution is therefore not that critical. Part of the numerical investigation would be to examine the effect of the height of the wall representing the power station buildings.

The wall part of the western boundary is treated just like any other solid wall. For the wind part of the boundary it is assumed that the pressure gradient normal to the boundary is zero and that the temperature is equal to the ambient temperature at that elevation. The turbulence quantities are extremely difficult to specify on this portion of the boundary. The wake of wind blowing around the boiler house will no doubt contain large turbulent eddies. It is very difficult to quantify this in the 2-D approximation on the given domain, as the normal turbulence equations for atmospheric turbulence are no longer applicable. Once again, however, the isolation of the major part of the domain from this boundary by the buoyant plume does render this less important. Numerical experiments showed that the actual turbulence levels in this boundary does not significantly affect the flow pattern. For this reason an insignificant turbulence level

is assumed and the turbulence quantities are thus set to zero.

The two atmospheric boundaries, namely the northern and eastern boundaries, are the most interesting boundaries to appear in the problem. The strongly buoyant plume will exit the domain across the northern boundary, while the eastern section of the northern boundary as well as the eastern boundary fall within the induction area of the domain. The numerical treatment on these atmospheric boundaries must therefore be able to handle all flow conditions from strong outflow to moderate inflow. The strong outflow condition is easily treated by most approaches, but the moderate inflow condition is a particular difficult situation. The problem is that it is impossible to specify values for the velocities on the boundary without solving the problem first. Instead of solving two problems, the power station vicinity and the large atmospheric problem, and then interfacing the two, the authors [1] developed the half cell technique that uses the momentum and global continuity equations to compute the boundary velocities. It is assumed that the numerical boundaries in the induction area are sufficiently far away from the power station for the gradients in all the variables to be small. For reasons of numerical stability the gradients of the velocity and pressure normal to the boundary are set to zero. This is not fully correct since the induction region is cone-like in shape, but once again numerical experiments have shown that this makes little difference to the resulting flow pattern. The zero gradient assumption is also good for the plume when it crosses the boundary at almost right angles. As the plume leans more towards the horizontal, the accuracy of the assumption decreases, but it is still used for lack of a better description.

The half cell technique uses the standard L-wise discretization of the numerical domain except on the boundary. On the eastern boundary for example, the u control volume touching the boundary would have its eastern neighbour outside the domain, or at best on the boundary. The latter condition is applied by effectively positioning a cell of half width on the boundary. In the case of a zero normal velocity gradient the discrete problem then reduces to $a_P u_P = a_N u_N + a_S u_S + a_W u_W + S_c$, where a_P, a_N, a_S and a_W are obtained from the same UWDS equations as before. The effect is therefore to remove the dependence on u_E, which is no longer defined.

The temperature and turbulence quantities are specified using a combination of the gradient and ambient value method, although the assumed boundary condition is that the gradient is insignificant. If the flow is into the domain, the insignificant gradient implies that the temperature and turbulence level would be the ambient value outside the domain. When the flow is out of the domain it would be the value inside the domain just upstream of the boundary. For the inflow case the boundary temperature is therefore set equal to the ambient value for stationary air, while for the turbulence quantities an insignificant turbulence level is assumed. Note that the usual turbulence equations for wind are not applicable since the flow in the induction area is not a wind in the usual sense. For the outflow situation the boundary value is simply set equal to the value next to the boundary.

Although the temperature on the boundary does not influence the temperatures inside the domain directly in the outflow case, it is important to specify that value accurately, because the boundary density depends on it, resulting in a possible violation of overall mass conservation which must be corrected. It is therefore important that the boundary temperature does not jump between and internal temperature (T_{int}) and ambient temperature (T_{amb}) as a result of small fluctuations in the boundary velocity. For the case where the flow over the boundary is small, an interpolatory procedure is therefore used, the boundary temperature being:

$$T_{bnd} = W(u_{bnd})T_{int} + (1 - W(u_{bnd}))T_{amb}, \qquad (5)$$

where:

$$W(u_{bnd}) = \begin{cases} 1 & \text{if } u_{bnd} \geqslant u_{ba}, \\ \frac{1}{2}(1 + u_{bnd}/u_{ba}) & \text{if } -u_{ba} < u_{bnd} < u_{ba}, \\ 0 & \text{if } u_{bnd} \leqslant -u_{ba} \end{cases}$$

and where u_{bnd} is the velocity perpendicular to the boundary. It is shown in [1] that Equation (5) can be derived from the energy equation and that the value of u_{ba} can be prescribed in terms of the Peclet number on the boundary. This value of u_{ba}, however, is very small. To enhance numerical stability a value of 0.5 m s^{-1} was used.

A phenomenon that is impossible to describe fully, without resolving the flow pattern outside the computational domain as well, is large scale recirculation. Warm air, diverted from the edge of the plume, may reenter the domain in the induction zone, thereby making the ambient air temperature warmer than it would be for the still air case. It is assumed that for the major part of the boundary this is not the case, but very close to the edge of the plume this assumption does not hold true. While it remains buoyant, the plume entrains some air so that there is convection towards the plume that restricts heat conduction to the surrounding atmosphere. The air next to the plume that moves downwards will, however, have a temperature that is higher than the surrounding air as a result of small-scale recirculation and conduction. A "smear" region is therefore defined next to the plume where the temperature at the last node of upward flow (therefore the edge of the plume) is linearly interpolated over a distance of 5 m in the downwind direction (therefore the inflow section next to the plume) to the ambient temperature at that elevation. This is a relatively arbitrary specification, but a more detailed motivation in reference [1] justifies it in terms of the energy equation. The "smear" region has little effect on the flow pattern as a whole, but has desirable stability properties for the numerical procedure.

5. THE HEAT EXCHANGER STRUCTURE

The heat exchanger/wind wall assembly is not strictly speaking an internal boundary, but an extension of the western boundary. The treatment, however, is identical to that of a completely internal boundary. The problem of passive and active structures as internal boundaries is discussed in more detail in [1]. The treatment of the heat exchanger problem is also given as an example. For the

detail and motivation of the treatment, the reader is referred to [1].

The heat exchanger is modelled as a series of columns of two pressure control volumes each. It is assumed that no horizontal flow is found inside the heat exchanger structure, and $u = 0$ is enforced on the heat exchanger. The end of the heat exchanger is clearly indicated by the last zero u-node on the eastern wall of the last pressure control volume on the heat exchanger. It is assumed that the fans are operated in such a way that a constant vertical velocity is obtained. This velocity is enforced on the middle node of each column of three v-nodes found on the heat exchanger. The dominant source method of Patankar [3] is used for this purpose. This results in the uncoupling of the pressure on opposite sides of the v-node as is required from the assumption that the velocity is maintained. The useful work (W) done by the fan is easily computed from the propeller equation $W = Av\Delta p$, where Δp is the pressure rise across the fan, v the velocity through, and A the area of the fan. The heat exchanger panels are assumed to be located on the northern control volume boundary that forms the northern limit of the heat exchanger. All the heat transfer therefore takes place on this interface between the heat exchanger and the atmosphere. Using the logarithmic mean temperature difference (LMTD) equation it can be shown that the heat transferred per unit area (Q) is given by:

$$Q = \rho v C_p (T_{exc} - T_{in}) \left[1 - \exp\left(\frac{-U}{\rho v C_p} \right) \right]. \qquad (6)$$

T_{exc} is the heat exchanger temperature, which is assumed to remain constant, and T_{in} is the air temperature at the inlet of the heat exchanger. For the finned tube heat exchanger it has been empirically determined that the heat transfer coefficient is given by $U = 4000\sqrt{v/2}$. Once again the turbulence quantities are very hard to specify and for the lack of more accurate information it is assumed that the fans and heat exchanger are "invisible" to the turbulence quantities.

The wind wall is modelled as an infinitesimally thin solid wall extending upwards from the eastern boundary of the last pressure control volume on the heat exchanger assembly. The wind wall is assumed to be so thin that it can be modelled as consisting only of the eastern boundaries of a column of pressure control volumes, extending upwards from the last pressure control volume at the end of the heat exchanger. The no-slip condition is assumed and $u = 0$ is enforced, using the dominant source method. This uncouples pressures on opposite sides of the wind wall as required. Contrary to the u-nodes, which are defined on the wind wall, no v-nodes are defined on the wind wall and imaginary v-nodes have to be defined. Note, however, that in the discrete transport equation, the product of the imaginary v-node and the appropriate a coefficient (say a_v) is zero. A convenient way of implementing the imaginary nodes is to use the a_v to calculate the applicable a_P coefficients and then set $a_v = 0$. In this case it does not matter by which value a_v is multiplied, the product will still be zero, even if multiplied by that v-node as if the wind wall did not exist. This makes it possible to incorporate the existence of the wind wall into the a_P coefficients and no exception needs to be included in the solution procedures for the imaginary nodes.

The conduction of heat through the wind wall is unlikely to be significant compared to the convection heat transfer that would have taken place had the wind not been included. The rate determining factor is clearly the heat transfer through the boundary layer on the wind wall and since the conduction rate of the metal is so much higher than that of the air, the effective heat conduction coefficient on the wind wall is set equal to the heat conduction coefficient of air. For the turbulence quantities, the usual wall function approach of Launder and Spalding [4] is followed, replacing the $-\rho\varepsilon$ term in the k equation source term by:

$$-\rho\varepsilon = \frac{C_{\mu\alpha}\rho^2 k^2}{\tau_w} \frac{\partial v}{\partial x}.$$

Here τ_w is the wall shear and is calculated from algebraic equations as shown by Launder and Spalding [4]. The zero k value on the wind wall is modelled in the same way in which the zero velocity (v) on the wind wall is modelled by the imaginary node incorporated in the a_P coefficient. The ε value adjacent to the wind wall is given by:

$$\varepsilon = \frac{C_{\mu\alpha}^{3/4} k^{3/2}}{\kappa^2 x_w},$$

where κ is the von Karman constant, 0.41, and x_w is the distance from the wall. This value is enforced using the dominant source method.

6. NUMERICAL RESULTS

Parts of the numerically produced flow field for the power station problem is shown in Figs 3–5, where the arrows indicate the relative size and direction of the flow. The results were produced on a 65×50 numerical grid and area averaged to produce arrows large enough to be easily displayed. A wind speed of 2 m s^{-1} is assumed in Figs 3 and 4 and 10 m s^{-1} in Fig. 5. A ground temperature of 20°C, an environmental lapse rate of 0.0065°C m^{-1} and heat exchanger and wind wall dimensions as described previously are assumed.

The effect of upwind buildings is investigated by omitting all buildings higher than the heat exchanger as shown in Fig. 3 and by a solid wall extending 55 m above the heat exchanger, therefore 100 m from ground level, as shown in Figs 4 and 5. It is clear from the flow pattern that buildings shield the heat exchanger from the prevailing wind so that the plume is almost vertical behind the building and is then bent over downwind by the wind. In the case where the building is omitted the entire plume is inclined, but the overall shape and size of the plume are not significantly altered. In actual fact, the amount of recirculation is less in the case without the shielding buildings as can clearly be seen in Figs 3c and 4c, where isobars in the vicinity of the heat exchanger are shown. The lowest pressure is about −200 Pa. The lower isobars were omitted to prevent cluttering.

Figure 5 shows the flow patterns at a wind speed of 10 m s^{-1}. The catastrophic collapse of the plume is evident and the heat island is clearly visible in Fig. 5b. This phenomenon is the direct result of the 2-D assumption which models the buoyant plume as an impenetrable

obstacle to the wind. As the wind speed increases the pressure on the obstacle increases and at some stage it must collapse. Numerical experiments have shown this critical speed to be about 5 m s^{-1}. In practice, of course, this will not happen because the wind can blow around the plume. Furthermore, the wind does not blow steadily, and changes in the wind speed would tend to break up the heat island. At high wind speeds, however, it is probable that a significant amount of recirculation will take place, reducing the efficiency of the heat exchanger.

To quantify the amount of recirculation, the effectiveness of the heat exchanger is defined as the amount of heat transferred as a fraction of the amount of heat that would be transferred if air at ambient temperature is drawn through the heat exchanger. For the case with no buildings and a 2 m s^{-1} wind the effectiveness is 99.4% with the 10 m wind wall and 97.1% without the wind wall. With the buildings the effectiveness is 98.0% with the wind wall and 93.6% without the wind wall. The effectiveness in each of the above cases is representative for wind speeds from 0 to 4 m s^{-1}, the effectiveness increasing slightly with increasing wind speed. This increase in effectiveness is attributed to the extra momentum added to the plume by the wind, increasing the entrainment on the induction side of the plume and thereby decreasing the recirculation. In the case of the collapsed plume, the effectiveness is only 39% in the case of a 10 m s^{-1} wind, a 100 m building and a 10 m wind wall as shown in Fig. 5. Again this is representative of the collapsed plume case, with predicted effectiveness varying from 30% in the case of a 5 m s^{-1} wind with a 100 m building and no wind wall to 45% for a 10 m s^{-1} wind,

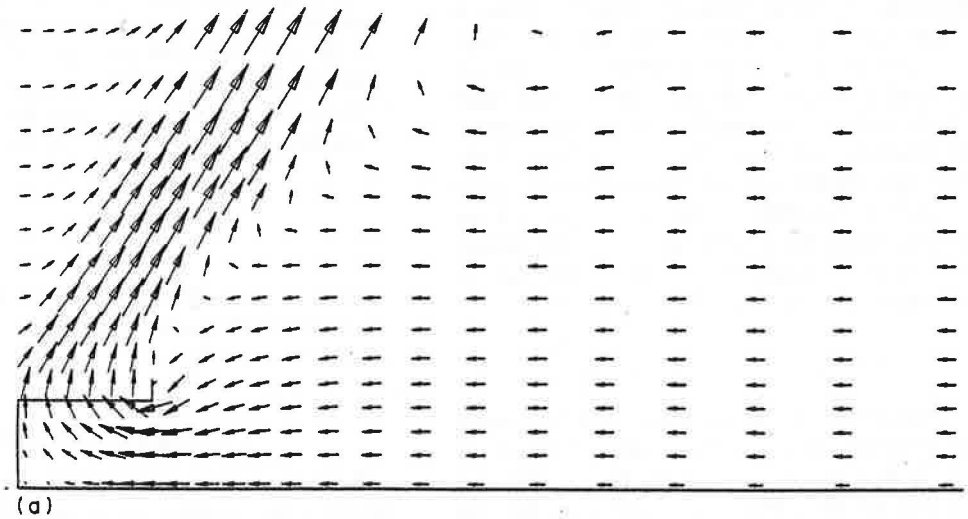

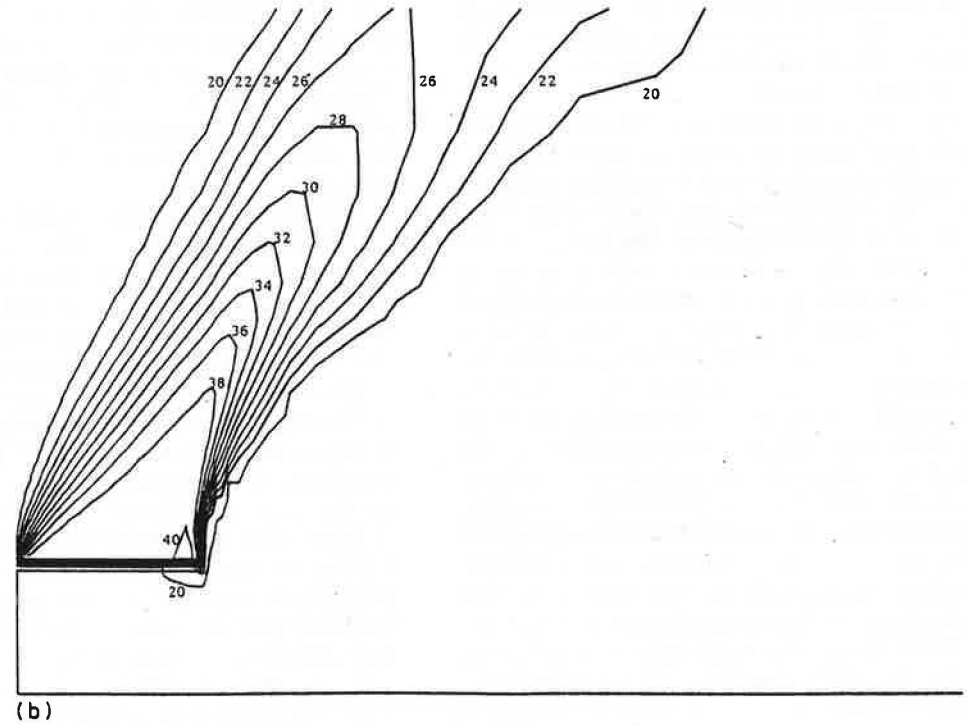

Fig. 3. (a) Flow field for low buildings in 2 m s^{-1} wind; (b) temperature profile for low buildings in 2 m s^{-1} wind; (c) isobars for low buildings in 2 m s^{-1} wind.

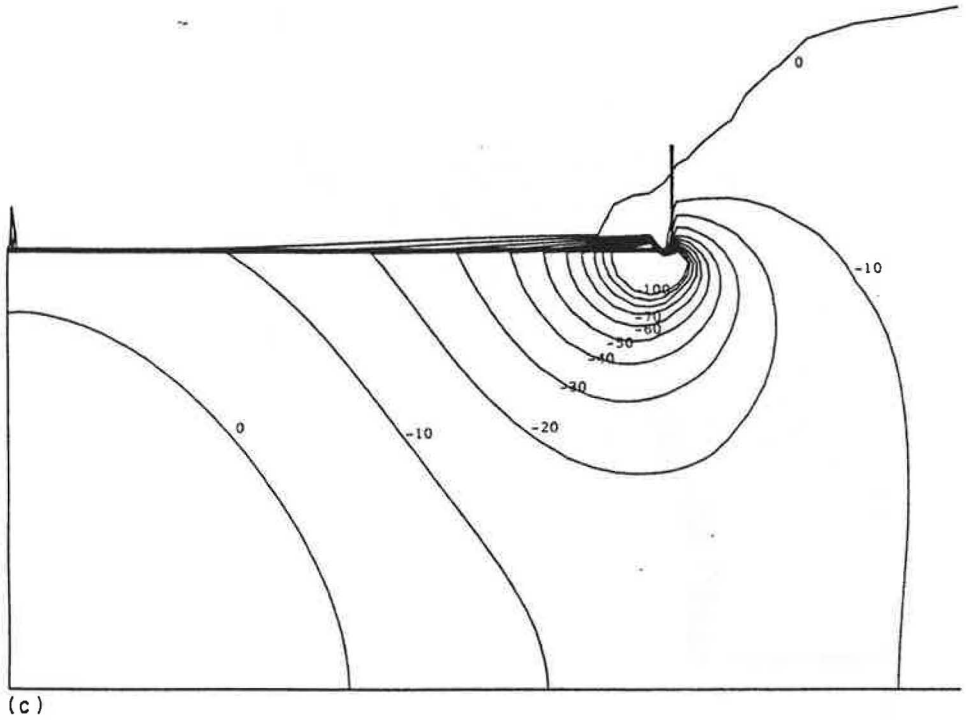

Fig. 3.—*continued.*

no building and a 10 m wind wall. The increase in effectiveness with wind speed for the collapsed plume is attributed to more effective heat transfer between the "heat island" and the flow passing over it at higher wind speeds. It should again be stressed that these are not accurate predictions, since it is an inherent shortcoming of the 2-D model, but it serves to illustrate what could happen in the 3-D case, presumably at a considerably higher wind speed.

Although it is not apparent from the flow patterns in Figs 3a and 4a, the flow on the eastern boundary of the domain has a vertical component that increases from 0 m s^{-1} at ground level to about 0.1 m s^{-1} downwards at an altitude of 250 m, while the horizontal component of the flow is about 2.5 m s^{-1} into the domain. The vertical velocity boundary condition is simply that the gradient on the boundary should be zero, which is implemented by setting the boundary vertical velocity equal to the

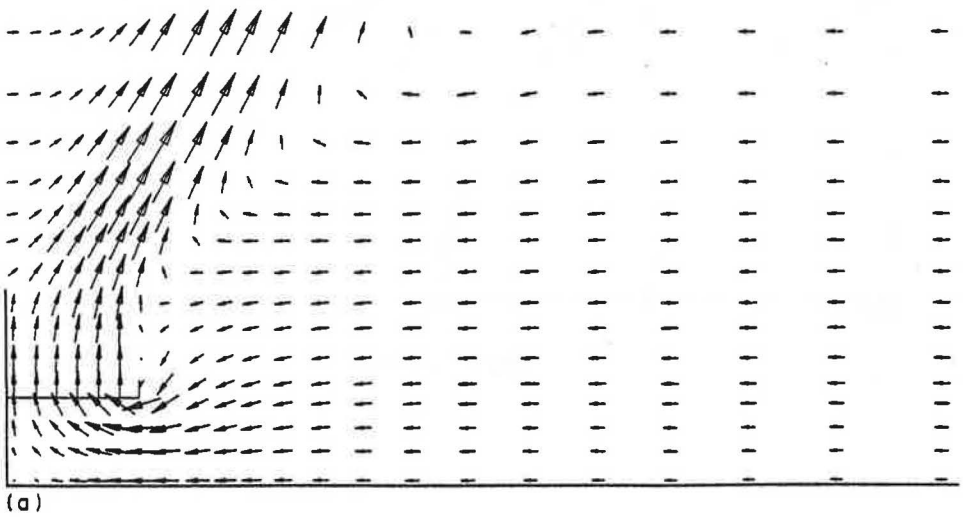

Fig. 4. (a) Flow field for high buildings in 2 m s^{-1} wind; (b) temperature profile for high buildings in 2 m s^{-1} wind; (c) isobars for high buildings in 2 m s^{-1} wind.

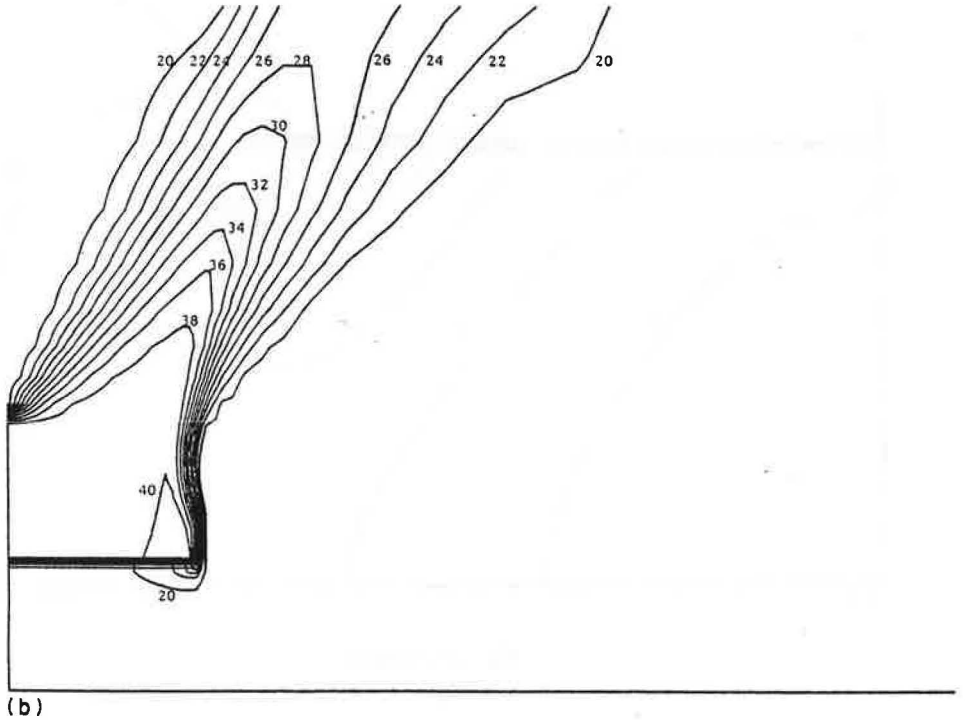

(b)

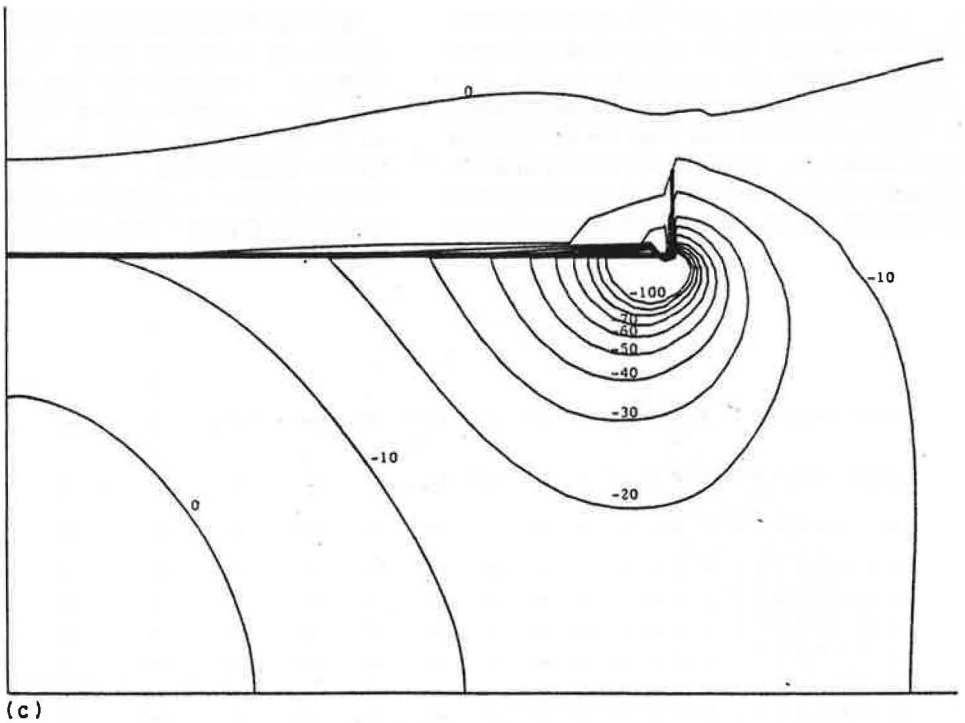

(c)

Fig. 4.—*continued.*

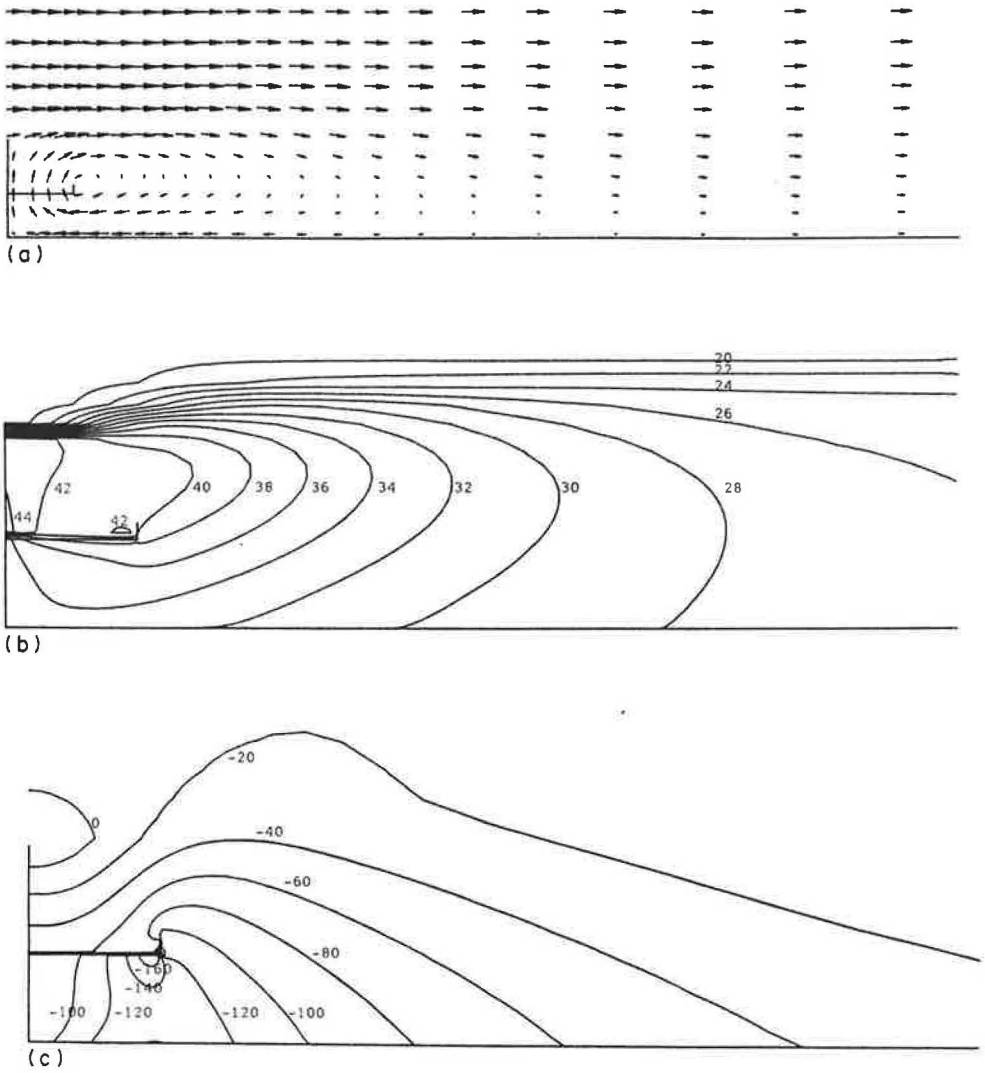

Fig. 5. (a) Flow field for high buildings in 10 m s^{-1} wind; (b) temperature profile for high buildings in 10 m s^{-1} wind; (c) isobars for high buildings in 10 m s^{-1} wind.

value just inside the domain. This attests to the effectiveness of the half cell method since such a situation is often numerically unstable.

7. CONCLUSIONS

The results shown in the previous section serve as proof of the practical applicability of the numerical method as described above. Although the method is not comprehensive, it is a practical way of obtaining reasonable solutions to a very complicated problem. The high wind speed solutions are obviously not representative of what happens in three dimensions. A full 3-D numerical investigation of the problem has therefore been launched. Fortunately the method vectorizes naturally and is therefore suitable for running on supercomputers.

As far as the design of power stations' heat exchangers or similar large heat dissipation devices are concerned, the JEEP code offers a tool that can be used to test modification of some design parameters such as, for example, the height of the wind wall, the heat exchanger temperature and wind speed that would otherwise be very difficult and expensive to accomplish.

Acknowledgement—The authors hereby gratefully acknowledge the assistance received and the computing facilities used at the University of Stellenbosch, where the major part of this work was conducted towards a PhD dissertation.

REFERENCES

1. W. A. Schreüder, Numerical prediction of air flow about a directly air cooled heat exchanger. PhD thesis, University of Stellenbosch (1986).
2. W. P. Jones and B. E. Launder, The calculation of low-Reynolds-number phenomena with a two-equation model of turbulence. *Int. J. Heat Mass Transfer* **16**, 1119–1130 (1973).
3. S. V. Patankar, *Numerical Heat Transfer and Fluid Flow*. Hemisphere, New York (1980).
4. B. E. Launder and D. B. Spalding, The numerical computation of turbulent flows. *Comput. Methods Appl. Mech. Engng* **3**, 269–289 (1974).